Granulocyte-Macrophage Colony-Stimulating Factor Protects Dimethylnitrosamine-Induced Rat Liver Fibrosis By Inhibiting Transforming Growth Factor-β1 Signaling Pathway

Mrigendra Bir Karmacharya
Inha University College of Medicine
Binika Hada
Inha University College of Medicine
So Ra Park
Inha University College of Medicine
Kil Hwan Kim
Veterans Medical Research Institute, Veterans Health Service Medical Center
Byung Hyune Choi (bryan@inha.ac.kr)
Inha University College of Medicine

Research Article

Keywords: GM-CSF, DMN, α-SMA, TGF-β1, PPAR-γ, liver fibrosis

Posted Date: June 25th, 2021

DOI: https://doi.org/10.21203/rs.3.rs-637791/v1

Abstract

Granulocyte-macrophage colony-stimulating factor (GM-CSF) exerts several therapeutic pharmacological effects but its role in liver fibrosis has not yet been studied. The current study investigates the inhibitory effects of GM-CSF on dimethylnitrosamine (DMN)-induced liver fibrosis in rats. In this study, liver fibrosis was induced in Sprague-Dawley rats by intraperitoneal injections of DMN (10 mg/kg of body weight) for three consecutive days per week for four weeks. To see the inhibitory effects on disease onset, GM-CSF (50 µg/kg of body weight) was injected for 2 consecutive days per week for 4 weeks along with DMN, while to see the therapeutic effects on disease progression, the GM-CSF injection was set forth at 4 weeks after the DMN injection. We found that DMN administration produced characteristics of molecular and pathological manifestations of liver fibrosis in rats including increased expressions of collagen I, alpha-smooth muscle actin (α-SMA), and transforming growth factor beta 1 (TGF-β1), and decreased PPAR-γ expression. Similarly, elevated serum levels of aspartate aminotransferase (AST), total bilirubin level (TBIL), and decreased albumin level (ALB) were observed. Treatment with GM-CSF improved the pathological liver conditions and significantly inhibited the elevated AST and TBIL, and increased ALB serum levels to normal. GM-CSF significantly decreased collagen I, α-SMA, and TGF-β1 expression and increased peroxisome proliferator-activated receptor gamma (PPAR-γ) expression. In conclusion, GM-CSF reduced the DMN-induced rat liver fibrosis by inhibiting TGF-β1 signaling pathway.

Introduction

Liver fibrosis – caused by chronic liver injuries – is one of the major causes of mortality worldwide[1]. A global study has reported that liver fibrosis accounted for 2.2% of death worldwide[2]. Liver fibrosis is a wound-healing response to chronic liver injuries resulting in excessive accumulation of extracellular matrix (ECM) proteins in hepatic tissues. Progressive liver fibrosis advances to cirrhosis, liver failure, and portal hypertension eventually leading to hepatic dysfunction[3]. Various etiologies such as chronic viral hepatitis, fat accumulation, alcoholic and non-alcoholic hepatic injuries, and toxin/drug-induced metabolic or autoimmune diseases that trigger reiterative damage to liver tissue have been implicated in liver fibrosis [4,5]. Dimethylnitrosamine (DMN) is a well-known hepatotoxin for inducing liver fibrosis in rats[6]. The DMN-induced liver fibrosis model closely resembles liver damage development in humans which includes nodular regeneration, ascites, ECM deposition, biochemical alterations, and histopathological manifestations[7].

Pathophysiologically, chronic hepatic injuries initiate the production of various fibrogenic cytokines in the liver tissue. Continued production of fibrogenic cytokines, such as target transforming growth factor-beta (TGF-β), connective tissue growth factor (CTGF), and platelet-derived growth factor (PDGF), transdifferentiates the quiescent nonparenchymal HSCs into fibrogenic myofibroblast-like cells[8]. Phenotypic transformation of HSCs into active myofibroblast-like proliferative state triggers the production of a massive amount of ECM proteins, primarily fibrillar collagens, fibronectin, and α-SMA; and ultimately leads to hepatic fibrosis[9-11]. Activated HSCs are also responsible for the proliferation and

migration of phenotypically transformed fibroblasts and the binding of TGF-β1 to its receptor that triggers the migration of such fibroblasts[12]. The binding of TGF-β1 with the type II receptor results in recruitment and phosphorylation of the type I receptor and phosphorylates Smad2 or Smad3 downstream. Phosphorylated Smad2 and Smad3 bind to Smad4 to form a heterotrimeric complex. This complex translocates to the nucleus and transcribes genes involved in ECM synthesis and deposition[13]. Owing to the importance of TGF-β signaling, ECM synthesis, and HSCs transformation in liver fibrosis pathophysiology, several anti-fibrotic strategies that target the ECM[14] and HSCs[15], and stem cell-based therapies[16] that target TGF-β1[17] and enhance anti-fibrotic efficacy[18] are the state-of-the-art therapeutic modalities for the treatment of liver fibrosis.

Granulocyte-macrophage colony-stimulating factor (GM-CSF) is a multipotent cytokine synthesized by many cell types, including macrophages, lymphocytes, fibroblasts, and endothelial cells[19]. GM-CSF has been implicated in a multitude of biological functions such as chemotaxis of inflammatory cells to wound sites[20]; proliferation and differentiation of early hematopoietic progenitor cells[21], epithelial regeneration[21], and wound-healing and neovascularization[22]. GM-CSF plays a complex tissue-dependent role in fibrosis[23], and has antiviral and immunoregulatory effects in patients with chronic hepatitis B[24]. GM-CSF has shown hepatic regeneration after 70% hepatectomy by promoting the hepatocellular DNA synthesis in a rat model[25].

Previously, we have demonstrated that GM-CSF inhibits glial formation and exhibits a long-term protective effect after spinal cord injury[26]. Additionally, we have shown that GM-CSF offers therapeutic potential for the remodeling of vocal fold (VF) wounds and the promotion of VF regeneration[20], and in the mobilization of bone marrow mesenchymal stem cells stimulation[27]. Furthermore, our previous study showed that GM-CSF inhibited the TGF-β-induced Rho-ROCK pathway and also rescued excessive collagen production *in vivo*[28]. In the present study, we developed a DMN-induced liver fibrosis in rats and examined the antihepatofibrotic effects of GM-CSF on liver fibrosis. The underlying molecular mechanisms of GM-CSF in reducing liver fibrosis are discussed.

Materials And Methods

Chemicals and Antibodies

Dimethylnitrosamine (DMN) was purchased from Wako Pure Chemical Industries (147-03781, Richmond, VA, USA). GM-CSF was obtained from Cure Cell (Ilsan, South Korea). Anti-collagen I antibody (ab34710), anti-alpha smooth muscle actin (α-SMA) antibody (ab5694), and goat anti-rabbit IgG H&L (HRP) antibody (ab205718) were purchased from Abcam (Cambridge, MA, USA). Anti-β-actin antibody (sc-47778) was purchased from Santa Cruz Biotechnology (Santa Cruz, CA, USA); anti-transforming growth factor β1 (TGFβ1) antibody was purchased from Sigma (St. Louis, MO, USA); and anti-peroxisome proliferator-activated receptor gamma (PPAR-γ) antibody (A3409A) was purchased from Thermo Fisher Scientific (Waltham, MA, USA).

Experimental design

The study was carried out **in compliance with the ARRIVE guidelines** (https://arriveguidelines.org). The experimental protocols for the animal study were approved by the Inha University Institutional Animal Care and Use Committee (INHA-IACUC, approval ID: INHA 170228-484-2) on their ethical procedures and scientific care. All the animals were treated strictly following the approved protocols. Sixty male Sprague-Dawley rats (8 weeks, 300 g) were purchased from Orient-Bio (Gyeonggi-do, South Korea). Rats were housed in a pathogen-free animal facility under 12 h light/dark cycle at constant temperature and humidity throughout the experiment. All rats were fed with standard rat chow with access to tap water *ad libitum*. After a week of acclimatization, the rats were assigned randomly into six groups (n = 10 for each group). Liver fibrosis was induced in the rats by intraperitoneal (IP) injection of DMN (10 mg/kg body weight). DMN was administered for the initial four weeks (three alternative days per week) and sacrificed either after 4 or 8 weeks after DMN administration.

For GM-CSF treatment, a group of DMN-injected rats received GM-CSF (50 μg/kg body weight, IP injection) right from the day of DMN administration for four weeks (two alternative days per week). The other group received GM-CSF (50 μg/kg body weight, IP injection) only from the 5^{th} week after DMN administration. For the sham control group, an equal volume of saline (0.9%, IP injection) was injected. The experimental scheme is shown in **Figure 1** where various groups were assigned as follows:

1. Control-4w (administered saline for four weeks; sacrificed at the end of 4^{th} week);
2. DMN-4w (administered DMN for four weeks; sacrificed at the end of 4^{th} week);
3. DMN+GM-4w (administered DMN and GM-CSF for four weeks; sacrificed at the end of 4^{th} week);
4. Control-8w (administered saline for the initial four weeks; sacrificed at the end of 8^{th} week);
5. DMN-8w (administered DMN for the initial four weeks; sacrificed at the end of 8^{th} week);
6. DMN+GM-8w (administered DMN for the initial four weeks; treated with GM-CSF from the 5^{th} week until the subjects were sacrificed at the end of the 8^{th} week).

The body weight of each subject was measured three times a week plus one time shortly before excising out the liver from the anesthetized rats.

Serum biochemical analysis

Blood samples were collected from venous and arterial blood vessels and heart chambers after 4 or 8 weeks of DMN administration. After leaving the samples at room temperature for 30 min, blood samples were centrifuged at 3000 rpm for 10 min. The supernatant was collected and stored at −70^{o}C before further analysis. Blood serum was used to analyze aspartate aminotransferase (AST), albumin (ALB), and total bilirubin (TBIL) by spectrometry using commercially available kits.

Histopathological examination

On the final day of the experiment, the whole liver was excised from anesthetized rats and weighed. Tissue samples were fixed with 10% neutral formalin solution. Histopathological slides of the tissue samples were prepared by a certified histopathologist. Briefly, fixed liver samples were embedded in paraffin blocks and 5 µm thick sections were prepared. Paraffin-embedded sections were deparaffinized and processed for Sirius Red and hematoxylin-eosin (H&E) staining. H&E and Sirius Red staining have been employed to evaluate the progression of liver fibrosis[42,43].

Immunohistochemical examination

Thin liver tissue sections were prepared and mounted on slides, deparaffinized in xylene, and rehydrated in alcohol. The level of collagen I, α-SMA, TGF-β1, and PPAR-γ were determined by immunohistochemical staining using the corresponding primary antibodies for collagen type I, α-SMA, TGFβ1, or PPAR-γ at recommended concentrations according to the manufacturer's instructions.

Western blot analysis

Total protein was isolated from a part of liver tissues according to the manufacturer's instructions. Liver tissue was homogenized in 300 µL RIPA buffer [0.5% Nonidet P-40, 20 mM Tris-Cl (pH 8.0), 50 mM NaCl, 50 mM NaF, 100 µM Na_3VO_4, 1 mM dithiothreitol, 50 µg/mL phenylmethylsulfonyl fluoride] containing protease inhibitors. The homogenates were centrifuged at 13,200 rpm for 30 min at 4°C. Protein (30 µg) was separated by sodium dodecyl sulfate polyacrylamide gel electrophoresis (SDS PAGE) and electrotransferred to polyvinylidene difluoride (PVDF) membranes. The PVDF membranes were blocked with non-fat milk solution in Tris-buffered saline containing 0.1% Tween-20 (TBST) for 1 h at room temperature. The membranes were then incubated with primary antibody (α-SMA, collagen type I, TGFβ1, or β-actin) at recommended concentrations overnight at 4°C. After washing, the membranes were incubated with horseradish peroxidase (HRP)-conjugated anti-rabbit secondary antibody directed against the primary antibody for 1 h at room temperature. The membranes were detected by an enhanced Bio-Rad Western blot detection system (Bio-Rad Laboratories, Hercules, CA, USA).

Image analysis

The prepared histopathological or immunohistological slides were examined under a microscope (DMi8, Leica Microsystems Inc., Buffalo Grove, IL, USA). The acquired images were analyzed quantitatively using ImageJ software[44]. Briefly, the acquired images (n = 5 for each group) were deconvoluted and threshold adjusted. The percentage expression of the appropriate color was calculated and the averaged value (± standard error of means, SEM) was presented.

Statistical analysis

Statistical analysis Statistical analyses were performed using SPSS software (IBM SPSS Statistics, IBM Corp., Armonk, NY, USA). Data for each experimental group was presented as the means ± SEM (standard error of means). Statistical significance. To test whether there were any statistically significant

differences between the means (± SEM) of the independent groups, one-way analyses of variance (ANOVA) were performed followed by Tukey's test as a *post hoc* test. Statistical significance was represented as *** for $p \leq 0.001$, ** for $p \leq 0.01$ and * for $p \leq 0.05$, and ns (not significant).

Results

GM-CSF reduced DMN-induced hepatofibrosis

Administration of DMN significantly induced hepatofibrotic changes in liver tissue in both the 4- and 8-week treatment groups. A qualitative examination of H&E-stained slides showed that DMN injection induced distinct changes in cellular architecture of liver tissue exhibiting formation of fibrotic bands – typical of the fibrotic liver – in DMN-4w (**Figure 2**) and DMN-8w (**Figure 3**) groups. Such fibrotic bands were absent in the corresponding sham-treated control groups. Additionally, the liver sections of the DMN-4w and DMN-8W groups exhibited abnormal arrangement of hepatic plates, infiltration of inflamed cells, collagen fiber deposition, and occurrence of fibrosis (**Figures 2** and **3**). Sham controls showed normal lobular architecture with structurally intact hepatic lobules and an orderly arrangement of hepatic plates (**Figures 2** and **3**). DMN-induced hepatofibrosis was further confirmed by a higher expression of hepatic collagen in Sirius Red staining. Sirius Red-staining demonstrated that DMN treatment increased extracellular collagen deposition in the liver tissue in both the 4- and 8-week treatment groups (**Figures 2** and **3**). Furthermore, immunohistochemical staining also showed a marked increase in collagen I and α-SMA expression in the DMN-treated groups. Both the 4- and 8-week treatment groups demonstrated a significantly higher expression of collagen I and α-SMA-positive cells as compared with the corresponding sham-treated control groups (**Figures 2** and **3**).

Treatment with GM-CSF recovered the DMN-induced liver damage in both the 4- and 8-week treatment groups. The H&E staining showed reappearance of the normal arrangement of the hepatic plates, reduction in infiltration of inflamed cells, and decrease in the thickening of collagen bundles in the GM-CSF-treated groups (**Figures 2** and **3**). Sirius Red staining also confirmed the reduction in collagen deposition by GM-CSF treatment. Consistent with the Sirius staining results, GM-CSF treatment significantly suppressed the expressions of collagen I and α-SMA induced by DMN in both the 4- and 8-week treatment groups (**Figures 2** and **3**).

Quantitatively, the folds-increase in the Sirius-Red-positive cells for the DMN- vs. DMN+GM-CSF-treated groups was 22.58 (± 0.59) vs. 3.52 (± 0.46) in the 4-week; and 18.36 (± 1.44) vs. 3.69 (± 0.18) in the 8-week treatment groups as compared with the corresponding sham-treated control groups (**Figure 4A**). The increase in Sirius-Red-positive cells be DMN treatment was statistically significant for both the 4- and 8-week DMN-treated groups ($p \leq 0.001$), and the decrease in Sirius-Red-positive cells in the DMN vs. DMN+GM groups was statistically significant for both the 4- and 8-week treatment groups ($p \leq 0.001$).

Likewise, there was a 28.10 (± 1.16) vs. 2.71 (± 1.16) and 19.68 (± 1.34) vs. 2.69 (± 1.34) folds increase in collagen I expression in the DMN- vs. DMN+GM-CSF-treated groups for the 4- and 8-week treatment groups, respectively, as compared with the corresponding sham-treated control groups (**Figure 4B**).

Expression of α-SMA, too, was increased by 15.21 (± 1.15) and 11.84 (± 0.59) folds and in the 4- and 8-week-DMN-treated groups respectively as compared with the corresponding control groups, which dropped down to 1.67 (± 0.09) and 1.48 (± 0.26) folds respectively in the GM-CSF-treated groups (**Figure 4C**). The increase in collagen I and α-SMA expression levels in the DMN-treated groups vs. control groups were statistically significant ($p \leq 0.001$), and the decrease in collagen I and α-SMA expression in DMN vs. DMN+GM groups were statistically significant for both the 4- and 8-week treatment groups ($p \leq 0.001$).

GM-CSF reduced DMN-induced liver damage and inhibited hepatotoxicity

Qualitative visual inspection of the excised livers showed that the liver lobes of the sham-treated control rats were brown, smooth, and soft with an evident glossy surface (**Figure 5A**). By contrast, the surface of the DMN-treated livers was rough, coarse, hard, and shrunken with dark discoloration. However, liver morphology of the GM-CSF-treated group showed a relatively smoother surface, an enhanced brown texture without scars, and rendered a similar liver texture as that of the sham-treated rats. Quantitatively, the 4- and 8-week DMN-injected rats showed a significant decrease in liver weight. The average weight of the liver was 3.91 (± 0.09) g in Control-4w vs. 2.94 (± 0.15) g in DMN-4w groups and 3.87 (± 0.06) g in Control-8w vs. 2.66 (± 0.23) g in DMN-8w groups. The percentage decrease in liver weight was 24.85 (± 1.13) % and 25.91 (± 1.28) % in the DMN-4w and DMN-8w groups, respectively, compared with the corresponding sham-treated control groups (**Figure 5B**). GM-CSF significantly improved the DMN-induced liver weight loss. The average weight of the liver was 3.58 (± 0.1) g in DMN+GM-4w and 3.52 (± 0.12) g in DMN+GM-8w groups. The percentage decrease in liver weight was only 11.18 (± 1.12) % and 9.94 (± 1.08) % in the DMN+GM-4w and DMN+GM-8w groups, respectively, as compared with the corresponding sham-treated control groups. The reduction of liver weight loss by GM-CSF was statistically significant in both DMN-4w vs. DMN+GM-4w and DMN-8w vs. DMN+GM-8w groups.

GM-CSF improved DMN-induced liver dysfunction

Biochemical analyses of the liver function showed that the DMN-treated rats in both the 4- and 8-week treatment groups developed hepatic injuries as evidenced by significantly higher concentrations of AST and TBIL and a significantly lower concentration of ALB compared with the sham-treated control rats (**Figure 6**). GM-CSF treatment recovered the DMN-induced liver dysfunction in both the 4- and 8-week treatment groups. Quantitatively, the average (± SEM) concentration of AST (U/L) for the Control-4w, DMN-4w, and DMN+GM-4w were respectively 105.8 (± 8.36), 200.9 (± 30.97), and 125.4 (± 12.07), and that for Control-8w, DMN-8w, and DMN+GM-8w were respectively 100.6 (± 7.25), 215.2 (± 11.20), and 126.7 (± 11.88) (**Figure 6A**). The difference in the average (± SEM) concentration of AST (U/L) between Control-4w vs. DMN-4w ($p \leq 0.01$), DMN-4w vs. DMN+GM-4w ($p \leq 0.05$), Control-8w vs. DMN-8w ($p \leq 0.001$), and DMN-8w vs. DMN+GM-8w ($p \leq 0.01$) were all statistically significant, while that between Control-4w vs. DMN+GM-4w, and between Control-8w vs. DMN+GM-8w were both statistically non-significant.

Similarly, the average (± SEM) concentration of TBIL (mg/dL) for Control-4w, DMN-4w, and DMN+GM-4w were respectively 0.18 (± 0.05), 0.88 (± 0.08), and 0.39 (± 0.06), and that for Control-8w, DMN-8w, and

DMN+GM-8w were respectively 0.14 (± 0.03), 0.69 (± 0.17), and 0.27 (± 0.05) (**Figure 6B**). The difference in the average (± SEM) concentrations of TBIL (mg/dL) between Control-4w vs DMN-4w ($p \leq 0.001$), DMN-4w vs DMN+GM-4w ($p \leq 0.01$), Control-8w vs DMN-8w ($p \leq 0.01$), and DMN-8w vs DMN+GM-8w ($p \leq 0.05$) were all statistically significant, while that between Control-4w vs. DMN+GM-4w, and between Control-8w vs DMN+GM-8w were both statistically non-significant.

The average (± SEM) concentration of ALB (g/dL) for Control-4w, DMN-4w, and DMN+GM-4w were respectively 3.14 (± 0.04), 2.33 (± 0.09), and 3.06 (± 0.11), and that for Control-8w, DMN-8w, and DMN+GM-8w were respectively 3.13 (± 0.04), 2.29 (± 0.15), and 2.79 (± 0.08) (**Figure 6C**). The difference in the average (± SEM) concentrations of TBIL (mg/dL) between Control-4w vs DMN-4w ($p \leq 0.001$), DMN-4w vs DMN+GM-4w ($p \leq 0.001$), Control-8w vs DMN-8w ($p \leq 0.001$), and DMN-8w vs DMN+GM-8w ($p \leq 0.05$) were all statistically significant, while that between Control-4w vs DMN+GM-4w, and between Control-8w vs DMN+GM-8w were both statistically non-significant.

GM-CSF improved survival rate and increased body weight of DMN-treated rats

Control-4w and Control-8w groups showed 100% survival (**Figures 7A** and **7B**), but 40% of the rats died in the DMN-4w group, and 70% of the rats died in the DMN-8w group during the drug intervention process. Interestingly, GM-CSF treatment substantially increased the survival of the DMN-treated rats only in the 4-week group, but not in the 8-week group. The DMN+GM-4w group showed a 100% survival (**Figure 7A),** while the DMN+GM-8w group did not show any increase in survival (**Figure 7B**).

Additionally, the 4-week administration of DMN significantly decreased the bodyweight of rats. On average, DMN-4w group rats lost 11.38 (± 4.68) % of their body weight compared to the baseline, while the Control-4w group gained 19.46 (± 2.46) % weight over four weeks (**Figure 7C**). However, GM-CSF treatment prevented DMN-induced body weight loss. DMN+GM-4w group showed an 8.78 (± 1.46) % increase in body weight over four weeks of GM-CSF treatment. The average bodyweight of the rats in the DMN+GM-4w group, 350.8 (± 5.19) g, was significantly higher than those in the DMN-4w group, 289.17 (± 9.51) g, while their baseline weights were comparable, 322.5 (± 2.8) g and 326 (± 2.74) g respectively, (**Figure 7C**). Similarly, the 8-week DMN-injected group, too, showed a dramatic decrease, −11.33 (± 7.12) %, in body weight as compared to the baseline. GM-CSF significantly recovered the body weight lost by DMN injection in four weeks (**Figure 7D**). There was an increase in body weight after GM-CSF administration, but the increase was not statistically significant.

GM-CSF inhibited DMN-induced TGF-β1 expression

Qualitative visual assessment of immunohistochemical slides showed that DMN treatment significantly increased TGF-β1 expression, and GM-CSF treatment substantially lowered the DMN-induced increase in TGF-β1 expression in both the 4- and 8-week treatment groups (**Figure 8A**). Quantitatively, DMN administration increased TGF-β1 expression by 11.05 (± 0.16) and 11.34 (± 0.09) folds in the 4- and 8-week treatment-groups, respectively. TGF-β1 expression levels in GM-CSF-treated groups were comparable to those in the corresponding control groups in both the 4- and 8-week treatment groups

(**Figure 8B**). The difference in TGF-β1 expression levels between Control-4w and DMN-4w; and that between DMN-4w and DMN+GM-4w were statistically significant ($p \leq 0.001$), but the difference in TGF-β1 expression levels between Control-4w and DMN+GM-4w was not statistically significant. Similarly, for the 8-week treatment groups, the difference in TGF-β1 expression levels between Control-8w and DMN-8w; and between DMN-8w and DMN+GM-8w were statistically significant ($p \leq 0.001$), but the difference in TGF-β1 expression levels between Control-8w and DMN+GM-8w was statistically not significant.

Western blotting confirms the effects of GM-CSF

Western blotting results showed that DMN significantly increased the expression of Collagen I, α-SMA, and TGF- β1; and GM-CSF significantly decreased the DMN-induced expression of Collagen I, α-SMA, and TGF- β1 in both the 4- and 8-week groups (**Figure 9A**). Compared with the corresponding control groups, the folds-increase in Collagen I (**Figure 9B**), α-SMA (**Figure 9C**), and TGF-β1 (**Figure 9D**) between GM-CSF vs. DMN-treated groups were 3.45 (± 0.25) vs. 21.66 (± 0.65), 1.47 (± 0.27) vs. 6.47 (± 0.41), and 1.1 (± 0.15) vs. 2.4 (± 0.45) folds in 4-week groups, and 3.78 (± 0.37) vs. 15.32 (± 0.87), 1.53 (± 0.26) vs. 4.18 (± 0.44), and 1.16 (± 0.02) vs. 1.82 (± 0.14) folds in 8-week groups respectively.

GM-CSF improved DMN-induced decrease in PPARγ expression

DMN treatment significantly lowered PPARγ expression, and GM-CSF treatment markedly increased PPARγ expression in both the 4- and 8-week treatment groups (**Figure 10A**). Quantitatively, DMN administration decreased PPARγ expression by 0.71 (± 0.03) and 0.35 (± 0.02) folds in the 4- and 8-week treatment-groups, respectively. PPARγ expression levels in GM-CSF-treated groups were comparable to those in the corresponding control groups in both the 4- and 8-week treatment groups (**Figure 10B**). The difference in PPARγ expression levels between Control-4w and DMN-4w; and that between DMN-4w and DMN+GM-4w were statistically significant ($p \leq 0.001$), but the difference in PPARγ expression levels between Control-4w and DMN+GM-4w was not statistically significant. Similarly, for the 8-week treatment groups, the difference in PPARγ expression levels between Control-8w and DMN-8w, and that between DMN-8w and DMN+GM-8w were statistically significant ($p \leq 0.001$), but the difference in PPARγ expression levels between Control-8w and DMN+GM-8w was not statistically significant.

Discussion

DMN, a potent liver-specific toxin, has remained one of the popular chemicals to induce liver fibrosis in animal models. It has been shown that chronic administration of DMN to rats produced advanced liver fibrosis with diffuse nodularity, marked portal hypertension, and accumulation of ascites[29]. Repeated injections of DMN bring about abnormalities in the biochemical and pathological manifestations of liver injury leading to liver fibrosis. Liver disease produced by DMN has been shown to closely represent human liver fibrosis. In the current study too, DMN injection induced liver fibrosis in rats in both the 4- and 8-week treatment schemes. DMN-treated rat livers exhibited several crucial pathological features of liver fibrosis including hardened and shrunken dark livers with a rough surface, an abnormal arrangement of

hepatic plates, infiltrated inflamed cells, and collagen fiber deposition. In addition, serum biochemical indicators for liver inflammation such as AST, ALB, and TBIL were released into the bloodstream in DMN-treated rat livers.

The development and progression of liver fibrosis is a consequence of highly coordinated cellular and molecular processes that occur following chronic liver injuries subsequently leading to activation of the hepatic stellate cells (HSC). Activation of HSCs from its quiescent state is considered one of the hallmarks of hepatic fibrosis which induces accumulation of collagen and ECM deposition in the liver[30]. Further activation of HSCs, marked by highly upregulated α-SMA[31], leads to myofibroblast-like phenotype and deposit large quantities of extracellular matrix (ECM) components in the liver[32]. Chronic exposure of DMN also leads to the increment in the α-SMA deposition, a widely accepted marker of transactivation of HSCs to myofibroblasts[33]. In the current study too, DMN injections increased expression of Collagen I and α-SMA proteins in liver tissue in both the 4- and 8-week treatment groups indicating HSC activation.

TGF-β1 is one of the important cytokines which directly activates HSCs and incites the fibrotic process[34]. Pathophysiologically, upon activation, TGF-β1 binds to its receptors and initiates the SMAD-dependent and/or SMAD-independent signaling pathways downstream resulting in the expression of profibrotic genes such as those encoding α-SMA, ECM proteins, and secreted cytokines and growth factors leading to fibrosis[35]. DMN injection has been shown to activate TGF-β1 in rat liver[36]. Our data also show that DMN injection markedly increased TGF-β1 expression in rat livers in both the 4- and 8-week groups. Owing to the significance of TGF-β1 activation in liver fibrosis progression, inhibition of the TGF-β1 pathway has remained one of the therapeutic strategies for liver fibrosis[37].

GM-CSF has been shown to exert several therapeutic pharmacological effects but, to our knowledge, its role in liver fibrosis has not yet been studied. Based on our previous findings on GM-CSF-induced inhibition of TGF-β1-dependent collagen synthesis in vocal fold scarring in rabbits[28]. we hypothesized that GM-CSF might also inhibit TGF-β1-dependent liver fibrosis. Consistent with our hypothesis, GM-CSF substantially reduced TGF-β1 expression in rat liver induced by DMN injections in 4- and 8-week treatment groups. Confirmed by both immunohistochemical staining and Western blotting analyses, TGF-β1 expression was significantly lesser in GM-CSF-treated groups as compared with that in DMN-treated groups. Further confirming the antihepatofibrotic bioeffects of GM-CSF, we found that GM-CSF significantly recovered the DMN-induced decrease in PPARγ expression. Upregulation of PPAR-γ by GM-CSF is crucial because when PPAR-γ is activated/upregulated, it suppresses the inflammation and inhibits TGF-β1 signaling pathways leading to the inhibition of TGF-β1-induced increase in α-SMA and collagen type I expression levels and ultimately reduces the ECM deposition, which ameliorates hepatic fibrosis in the hepatic cells[38–40].

It has been reported that the accumulation of ECM proteins disturbs the liver architecture by forming a fibrous scar and the subsequent development of cirrhosis with nodules of regenerating hepatocytes, which often leads to progressive loss of liver function[3]. Hence, antifibrogenic therapy that suppresses the

activation of HSCs has been preferentially considered as an attractive target to prevent the pathological progression to cirrhosis in chronic liver diseases[41]. Our present data show that the number of α-SMA positive cells in the liver increased by DMN treatment were suppressed by GM-CSF administration and also suppressed the increased collagen accumulation. Taken together, these findings suggest that the antifibrotic effect of GM-CSF may be due to suppression of HSC activation. Moreover, GM-CSF inhibited the DMN-induced liver damage and hepatotoxicity, and also increased body weights and survival rate. The hepatoprotective effects of GM-CSF against DMN-induced hepatotoxicity were further confirmed by the prevention of liver weight loss resulted from DMN administration. Intraperitoneal injection of GM-CSF was able to keep the liver near to normal biomarker levels and reversed histological integrity.

It should, however, be noted that some rats died in the DMN + GM-8w group where DMN was injected alone for four weeks and GM-CSF was administered only from the beginning of the 5th week. But most of the rats that died were at the end of the 4th week following DMN administration which did not receive GM-CSF treatment. In the DMN + GM-4w group, on the other hand, where GM-CSF was administered together with DMN, GM-CSF considerably minimized the toxic effects of DMN.

Conclusion

In summary, our results confirm the inhibitory and therapeutic effects of GM-CSF against DMN-induced liver fibrosis in rats. The results showed that GM-CSF had some specific therapeutic effects on pathological changes in the liver. We demonstrated that GM-CSF act as antifibrogenic agent which significantly reduced the DMN-induced increase in collagen I and α-SMA expression by suppressing TGF-β1 expression and increasing PPAR-γ expression that ultimately suppressed the activation of HSCs. Hence, GM-CSF can be an attractive target to prevent/cure pathological progression to liver fibrosis and should studied further for its potent clinical applications.

Declarations

Acknowledgement

The authors would like to acknowledge Dr. Moon Hang Kim for his help and support during this study.

Financial support

The study was supported by a VHS Medical Center Research Grant (VHSMC17013) and the Inha University Research Grant (63000-01).

Conflict of interest

The authors declare that there is no conflict of interest.

Authors contributions

All authors made significant contributions to the study. MBK and BH conceptualized the study, performed experiments, acquired, analyzed, and interpreted data, and wrote the manuscript. SRP made technical comments on the experiments and revised the manuscript. KHK and BHC conceptualized the study, analyzed and interpreted data, and revised the manuscript.

References

1. Koyama, Y. & Brenner, D. A. Liver inflammation and fibrosis. *The Journal of clinical investigation*, **127**, 55–64 https://doi.org/10.1172/JCI88881 (2017).
2. Global and national age-sex specific all-cause and cause-specific mortality for 240 causes of death, 1990–2013: a systematic analysis for the Global Burden of Disease Study 2013., **385**, 117–171 https://doi.org/10.1016/S0140-6736(14)61682-2 (2015).
3. Bataller, R. & Brenner, D. A. Liver fibrosis. *J Clin Invest*, **115**, 209–218 https://doi.org/10.1172/JCI24282 (2005).
4. Hernandez-Gea, V. & Friedman, S. L. Pathogenesis of liver fibrosis. *Annu Rev Pathol*, **6**, 425–456 https://doi.org/10.1146/annurev-pathol-011110-130246 (2011).
5. Pinzani, M. Pathophysiology of Liver Fibrosis. *Dig Dis*, **33**, 492–497 doi:10.1159/000374096 [pii] (2015).
6. Chooi, K. F., Rajendran, K., Phang, D. B., Toh, H. H. & S. S. & The Dimethylnitrosamine Induced Liver Fibrosis Model in the Rat. *Journal of visualized experiments: JoVE*, https://doi.org/10.3791/54208 (2016).
7. George, J., Rao, K. R., Stern, R. & Chandrakasan, G. Dimethylnitrosamine-induced liver injury in rats: the early deposition of collagen., **156**, 129–138 doi:S0300483X00003528 [pii] (2001).
8. Tsukada, S., Parsons, C. J. & Rippe, R. A. Mechanisms of liver fibrosis. *Clin Chim Acta*, **364**, 33–60 https://doi.org/10.1016/j.cca.2005.06.014 (2006).
9. Lemoinne, S., Cadoret, A., El Mourabit, H., Thabut, D. & Housset, C. Origins and functions of liver myofibroblasts. *Biochim Biophys Acta*, **1832**, 948–954 https://doi.org/10.1016/j.bbadis.2013.02.019 (2013).
10. Moreira, R. K. Hepatic stellate cells and liver fibrosis. *Arch Pathol Lab Med*, **131**, 1728–1734 https://doi.org/10.1043/1543-2165(2007)131[1728:HSCALF]2.0.CO;2 (2007).
11. Gressner, A. M. & Weiskirchen, R. Modern pathogenetic concepts of liver fibrosis suggest stellate cells and TGF-beta as major players and therapeutic targets. *J Cell Mol Med*, **10**, 76–99 doi:010.001.07 [pii] (2006).
12. Ding, N. *et al.* A vitamin D receptor/SMAD genomic circuit gates hepatic fibrotic response., **153**, 601–613 https://doi.org/10.1016/j.cell.2013.03.028 (2013).
13. Hong, S. W. *et al.* Suppression by fucoidan of liver fibrogenesis via the TGF-beta/Smad pathway in protecting against oxidative stress. *Biosci Biotechnol Biochem*, **75**, 833–840

https://doi.org/10.1271/bbb.100599 (2011).

14. Schuppan, D., Ashfaq-Khan, M., Yang, A. T. & Kim, Y. O. Liver fibrosis: Direct antifibrotic agents and targeted therapies. *Matrix biology: journal of the International Society for Matrix Biology*, **68–69**, 435–451 https://doi.org/10.1016/j.matbio.2018.04.006 (2018).
15. Nathwani, R. *et al.* A Review of Liver Fibrosis and Emerging Therapies. *European Medical Journal*, **4**, 105–116 (2019).
16. Wang, J., Sun, M., Liu, W., Li, Y. & Li, M. Stem Cell-Based Therapies for Liver Diseases: An Overview and Update. *Tissue engineering and regenerative medicine*, **16**, 107–118 https://doi.org/10.1007/s13770-019-00178-y (2019).
17. Kao, Y. H. *et al.* Infusion of Human Mesenchymal Stem Cells Improves Regenerative Niche in Thioacetamide-Injured Mouse Liver. *Tissue engineering and regenerative medicine*, **17**, 671–682 https://doi.org/10.1007/s13770-020-00274-4 (2020).
18. Wang, X. *et al.* Erythropoietin-Modified Mesenchymal Stem Cells Enhance Anti-fibrosis Efficacy in Mouse Liver Fibrosis Model. *Tissue engineering and regenerative medicine*, **17**, 683–693 https://doi.org/10.1007/s13770-020-00276-2 (2020).
19. Shi, Y. *et al.* Granulocyte-macrophage colony-stimulating factor (GM-CSF) and T-cell responses: what we do and don't know. *Cell Res*, **16**, 126–133 https://doi.org/10.1038/sj.cr.7310017 (2006).
20. Lim, J. Y. *et al.* Regulation of wound healing by granulocyte-macrophage colony-stimulating factor after vocal fold injury. *PLoS One*, **8**, e54256 https://doi.org/10.1371/journal.pone.0054256 (2013).
21. Irons, R. D. & Stillman, W. S. Cell proliferation and differentiation in chemical leukemogenesis., **11**, 235–242 https://doi.org/10.1002/stem.5530110311 (1993).
22. Mann, A., Breuhahn, K., Schirmacher, P. & Blessing, M. Keratinocyte-derived granulocyte-macrophage colony stimulating factor accelerates wound healing: Stimulation of keratinocyte proliferation, granulation tissue formation, and vascularization. *J Invest Dermatol*, **117**, 1382–1390 https://doi.org/10.1046/j.0022-202x.2001.01600.x (2001).
23. Mann, A., Niekisch, K., Schirmacher, P. & Blessing, M. Granulocyte-macrophage colony-stimulating factor is essential for normal wound healing.*J Investig Dermatol Symp Proc***11**,87–92, doi:S0022-202X(15)52629-8 [pii] (2006)
24. Kountouras, J., Boura, P. & Tsapas, G. In vivo effect of granulocyte-macrophage colony-stimulating factor and interferon combination on monocyte-macrophage and T-lymphocyte functions in chronic hepatitis B leukocytopenic patients. *Hepatogastroenterology*, **45**, 2295–2302 (1998).
25. Eroglu, A. *et al.* Effect of granulocyte-macrophage colony-stimulating factor on hepatic regeneration after 70% hepatectomy in normal and cirrhotic rats. *HPB (Oxford)*, **4**, 67–73 https://doi.org/10.1080/136518202760378425 (2002).
26. Huang, X. *et al.* GM-CSF inhibits glial scar formation and shows long-term protective effect after spinal cord injury. *J Neurol Sci*, **277**, 87–97 https://doi.org/10.1016/j.jns.2008.10.022 (2009).
27. Kim, J., Kim, N. K., Park, S. R. & Choi, B. H. GM-CSF Enhances Mobilization of Bone Marrow Mesenchymal Stem Cells via a CXCR4-Medicated Mechanism. *Tissue engineering and regenerative*

medicine, **16**, 59–68 https://doi.org/10.1007/s13770-018-0163-5 (2019).

28. Choi, J. K. *et al.* GM-CSF reduces expression of chondroitin sulfate proteoglycan (CSPG) core proteins in TGF-beta-treated primary astrocytes. *BMB Rep*, **47**, 679–684 [pii] (2014).
29. Jenkins, S. A. *et al.* A dimethylnitrosamine-induced model of cirrhosis and portal hypertension in the rat. *J Hepatol*, **1**, 489–499 https://doi.org/10.1016/s0168-8278(85)80747-9 (1985).
30. Suarez-Cuenca, J. A. *et al.* Partial hepatectomy-induced regeneration accelerates reversion of liver fibrosis involving participation of hepatic stellate cells. *Exp Biol Med (Maywood)*, **233**, 827–839 https://doi.org/10.3181/0709-RM-247 (2008).
31. Nouchi, T., Tanaka, Y., Tsukada, T., Sato, C. & Marumo, F. Appearance of α-smooth-muscle-actin-positive cells in hepatic fibrosis., **11**, 100–105 https://doi.org/10.1111/j.1600-0676.1991.tb00499.x (1991).
32. Xu, J. *et al.* The types of hepatic myofibroblasts contributing to liver fibrosis of different etiologies. *Frontiers in pharmacology*, **5**, 167 https://doi.org/10.3389/fphar.2014.00167 (2014).
33. Tekkesin, N., Taga, Y., Sav, A. & Bozkurt, S. Modulation of extracellular matrix proteins and hepatate stellate cell activation following gadolinium chloride induced Kuffer cell blockade in an experimental model of liver fibrosis/cirrhosis. Vol 2013 (2013).
34. Bissell, D. M. Chronic liver injury, TGF-beta, and cancer. *Exp Mol Med*, **33**, 179–190 https://doi.org/10.1038/emm.2001.31 (2001).
35. Kim, K. K., Sheppard, D. & Chapman, H. A. TGF-beta1 Signaling and Tissue Fibrosis. *Cold Spring Harbor perspectives in biology*, **10**, https://doi.org/10.1101/cshperspect.a022293 (2018).
36. Kondou, H. *et al.* A blocking peptide for transforming growth factor-beta1 activation prevents hepatic fibrosis in vivo. *J Hepatol*, **39**, 742–748 https://doi.org/10.1016/s0168-8278(03)00377-5 (2003).
37. Liu, X., Hu, H. & Yin, J. Q. Therapeutic strategies against TGF-beta signaling pathway in hepatic fibrosis. *Liver international: official journal of the International Association for the Study of the Liver*, **26**, 8–22 https://doi.org/10.1111/j.1478-3231.2005.01192.x (2006).
38. Guo, B. *et al.* Peroxisome proliferator-activated receptor-gamma ligands inhibit TGF-beta 1-induced fibronectin expression in glomerular mesangial cells., **53**, 200–208 (2004).
39. Deng, Y. L., Xiong, X. Z. & Cheng, N. S. Organ fibrosis inhibited by blocking transforming growth factor-β signaling via peroxisome proliferator-activated receptor γ agonists. *Hepatobiliary & Pancreatic Diseases International*, **11**, 467–478 https://doi.org/10.1016/S1499-3872(12)60210-0 (2012).
40. Choi, J. H. *et al.* Capsaicin Inhibits Dimethylnitrosamine-Induced Hepatic Fibrosis by Inhibiting the TGF-beta1/Smad Pathway via Peroxisome Proliferator-Activated Receptor Gamma Activation. *J Agric Food Chem*, **65**, 317–326 https://doi.org/10.1021/acs.jafc.6b04805 (2017).
41. Zhang, C. Y., Yuan, W. G., He, P., Lei, J. H. & Wang, C. X. Liver fibrosis and hepatic stellate cells: Etiology, pathological hallmarks and therapeutic targets. *World journal of gastroenterology*, **22**, 10512–10522 https://doi.org/10.3748/wjg.v22.i48.10512 (2016).

42. Du, J. X. *et al.* Ingredients of Huangqi decoction slow biliary fibrosis progression by inhibiting the activation of the transforming growth factor-beta signaling pathway. *BMC complementary and alternative medicine*, **12**, 33 https://doi.org/10.1186/1472-6882-12-33 (2012).
43. Tung, Y. T. *et al.* Lactoferrin protects against chemical-induced rat liver fibrosis by inhibiting stellate cell activation. *J Dairy Sci*, **97**, 3281–3291 https://doi.org/10.3168/jds.2013-7505 (2014).
44. Schindelin, J., Rueden, C. T., Hiner, M. C. & Eliceiri, K. W. The ImageJ ecosystem: An open platform for biomedical image analysis. *Molecular reproduction and development*, **82**, 518–529 https://doi.org/10.1002/mrd.22489 (2015).

Figures

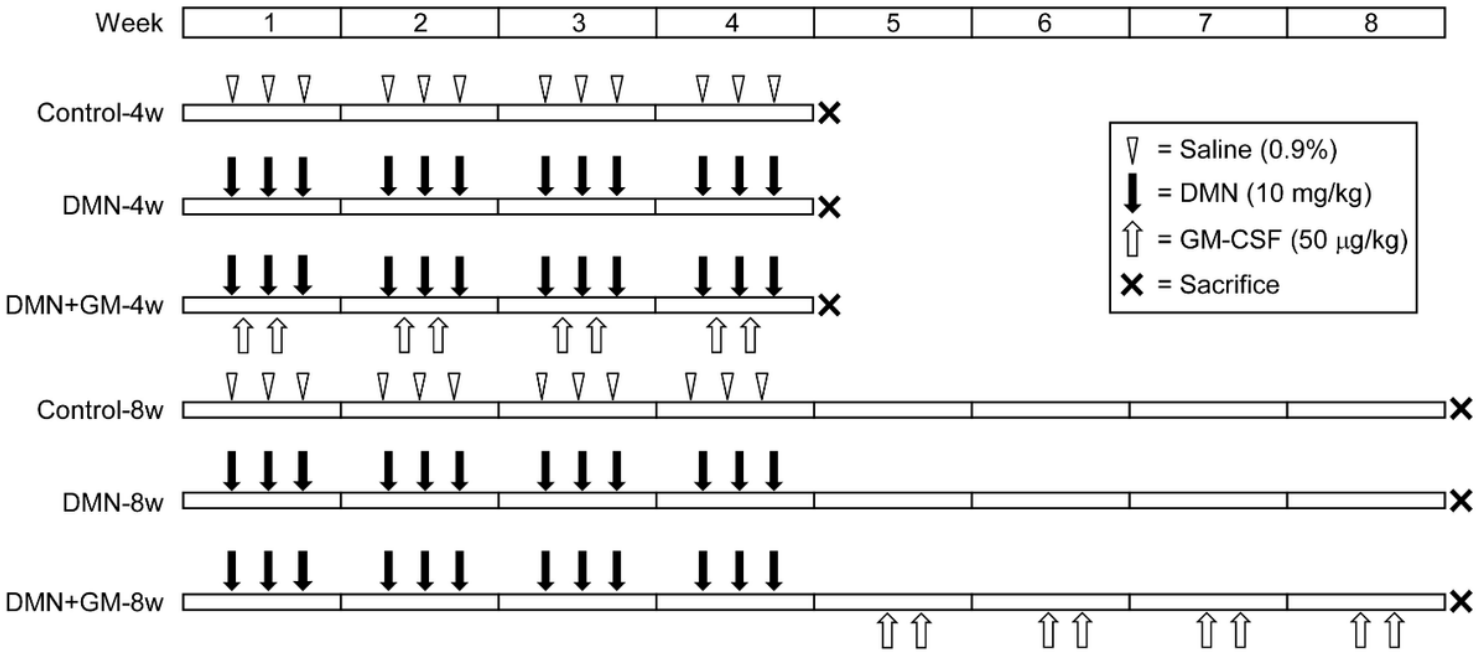

Figure 1

Schematic diagram of the experimental protocol. Rats were divided into six groups. Each group has ten rats (n = 10). Hepatic fibrosis was induced by administration of DMN (10 mg/kg body weight, IP injection) three times per week for four weeks. GM-CSF was administered in rats (50 μg/kg body weight, IP injection) two every other day for four weeks in DMN+GM-4w group. The DMN+GM-8w group received GM-CSF (50 μg/kg body weight, IP injection) two alternative days per week for four weeks only from the 5th week after DMN administration. Control groups were administered equivalent saline alone (0.9%) three times a week for four weeks via IP injection. Rats of the 4-week groups were euthanized on 29th day and 8-week groups on 55th day after the initial DMN administration.

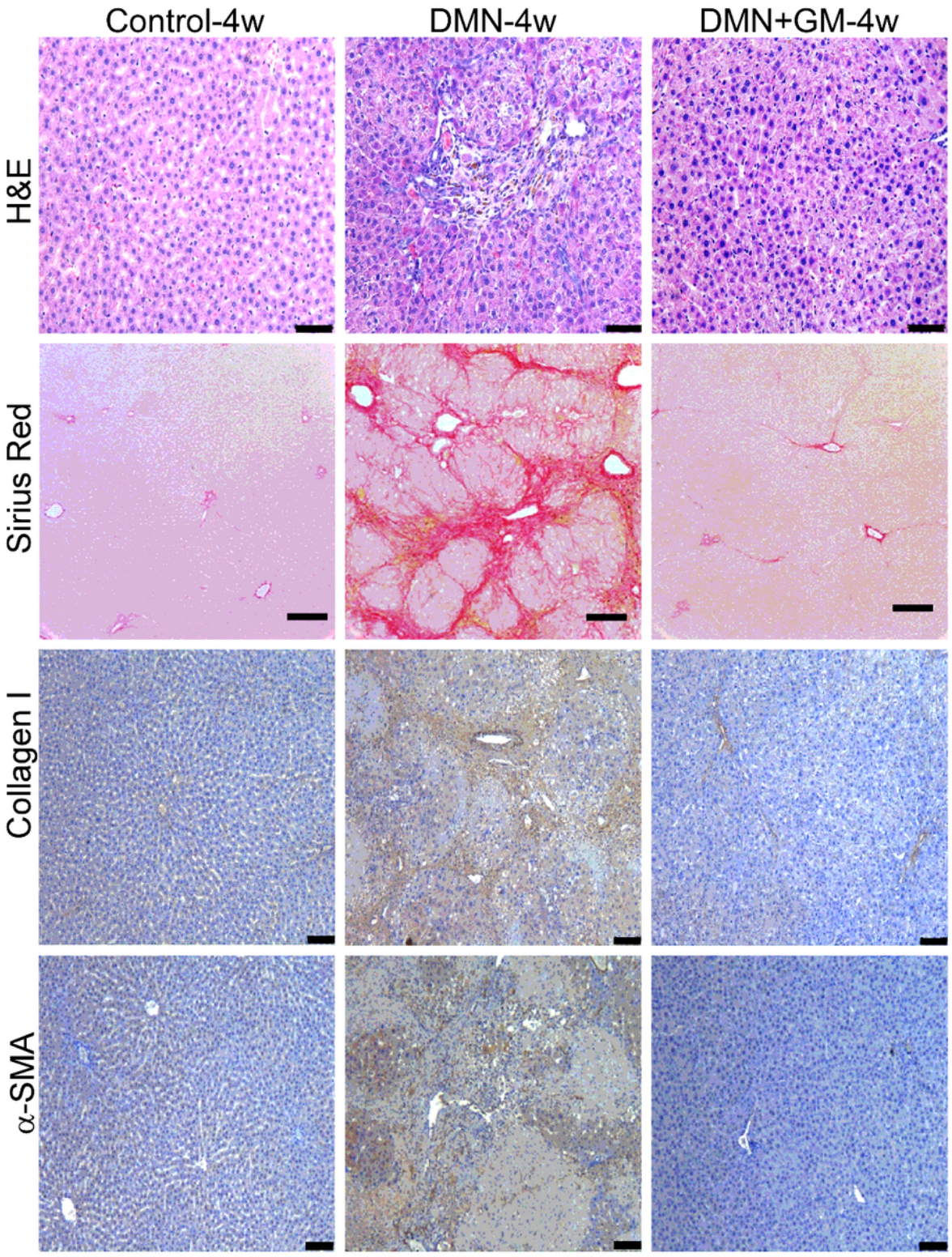

Figure 2

Effects of GM-CSF on DMN-induced histopathological changes in the 4-week group. Liver tissue was collected at the 29th day after the initial DMN administration and fixed in 10% neutral formalin solution. Thin sections (5 μm) were cut and stained with hematoxylin and eosin (H&E) and Sirius Red. Collagen I and α-SMA proteins were detected immunoshitochemically.

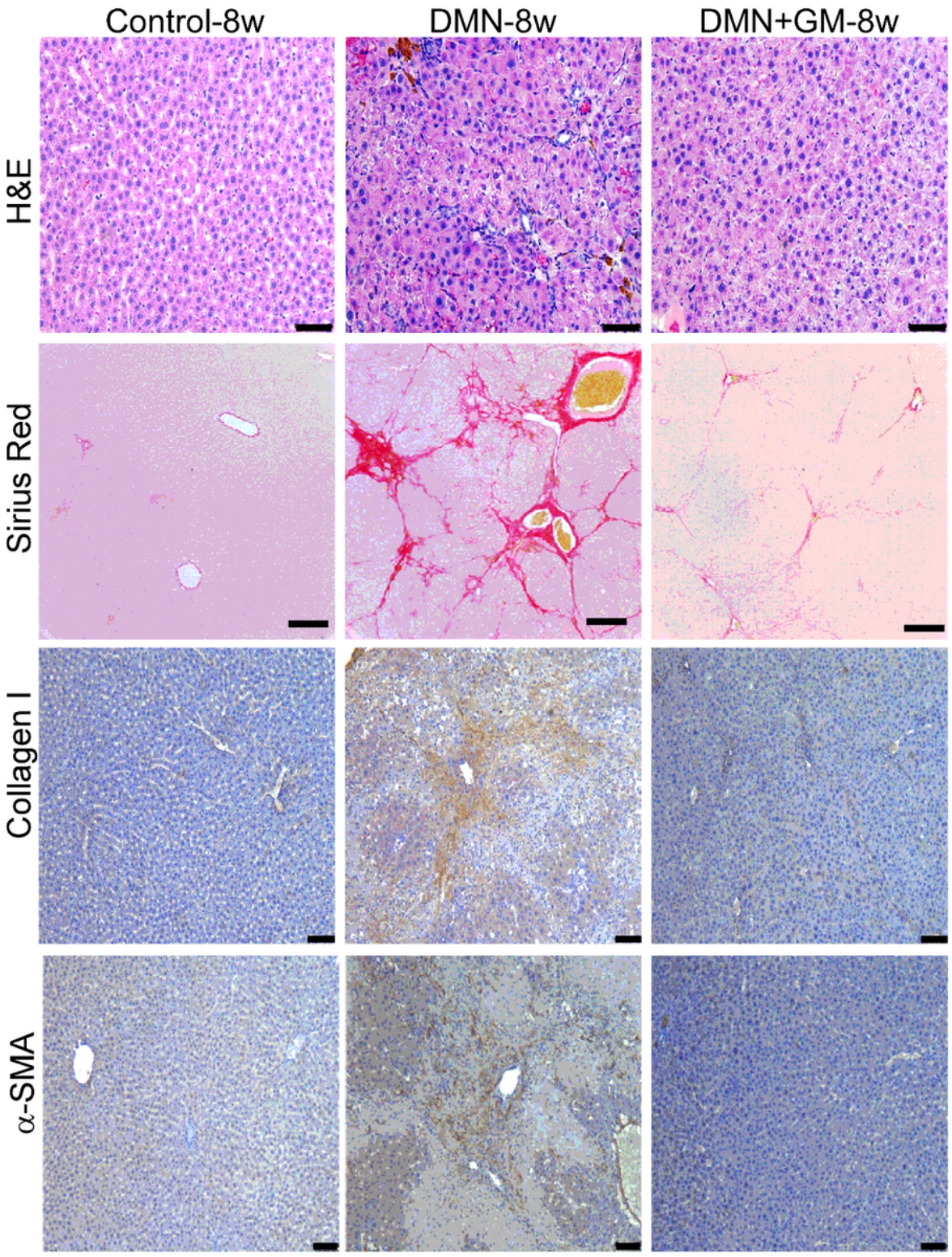

Figure 3

Effects of GM-CSF on DMN-induced histopathological changes in the 8-week group. Liver tissue was collected at the 57th day after the initial DMN administration and fixed in 10% neutral formalin solution. Thin sections (5 μm) were cut and stained with hematoxylin and eosin (H&E) and Sirius Red. Collagen I and α-SMA proteins were detected immunoshitochemically.

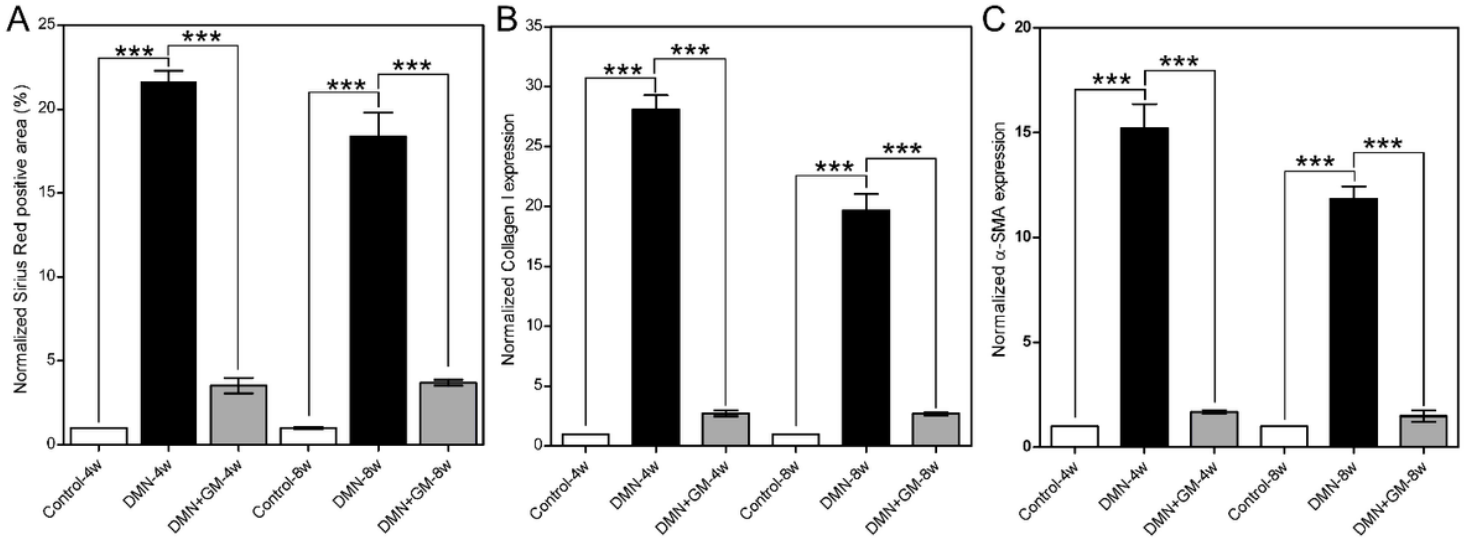

Figure 4

Quantification of the effects of GM-CSF on DMN-induced histopathological changes. (A) Sirius Red staining, (B) Collagen I content, and (C) α-SMA expression. Data were calculated from the liver tissue sections as represented in Figures 2 and 3. Colors from every images each for Sirius Red, Collagen I, and α-SMA prepared from each rat were separated by deconvolution and the intensity of each color per given area of each image for Sirius Red, Collagen I, and α-SMA were measured. The data were averaged and normalized with respect to the corresponding control groups and presented as the fold-change. Results are expressed as the means (± SEM). Statistical significance was assigned as *** for $p \leq 0.001$.

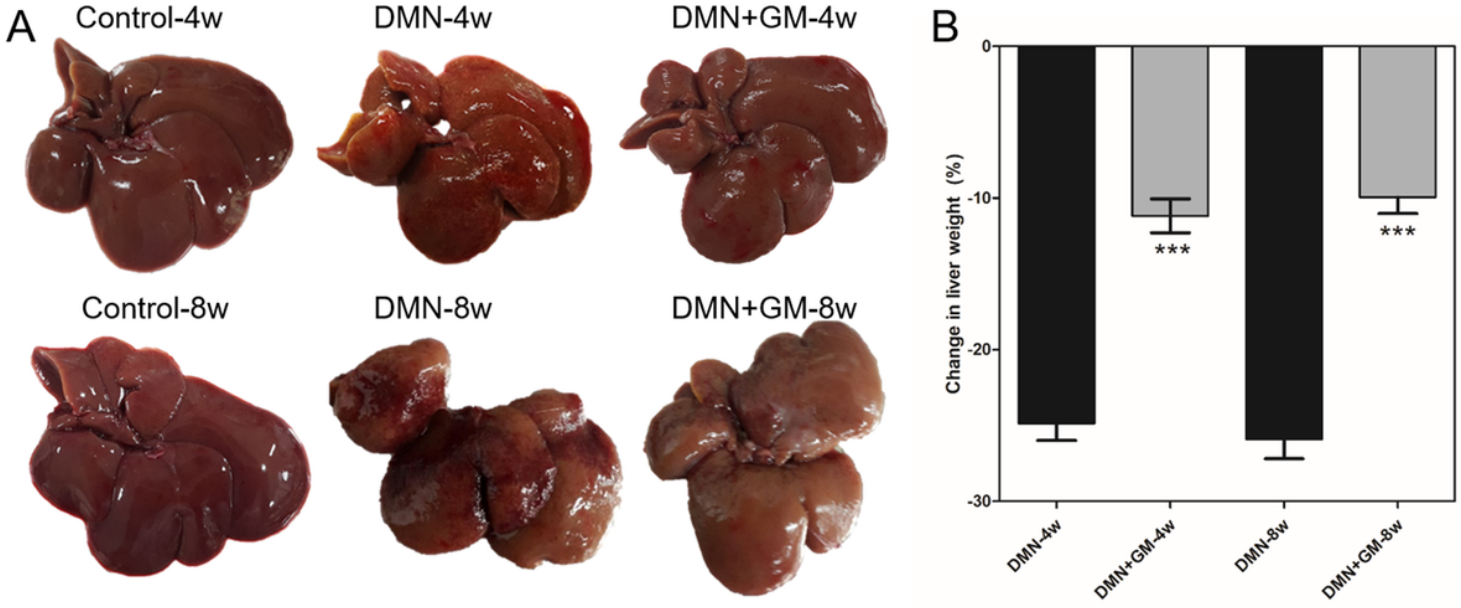

Figure 5

Effects of GM-CSF on DMN-induced changes in liver morphology, texture, and weight. (A) Images showing morphology and texture of liver lobes in control or DMN-treated rats with or without GM-CSF treatment. Note that DMN-treatment markedly changed the liver morphology and texture, and GM-CSF

treatment clearly improved the DMN-induced changes in liver morphology and texture in both the 4- and 8-week treatment groups. (B) Histograms showing changes in liver weight with respect to the corresponding controls by administration of DMN ± GM-CSF in rats. GM-CSF treatment significantly improved DMN-induced reduction in liver weight in both the 4- and 8-week treatment groups. Statistical significance was assigned as *** for $p \leq 0.001$.

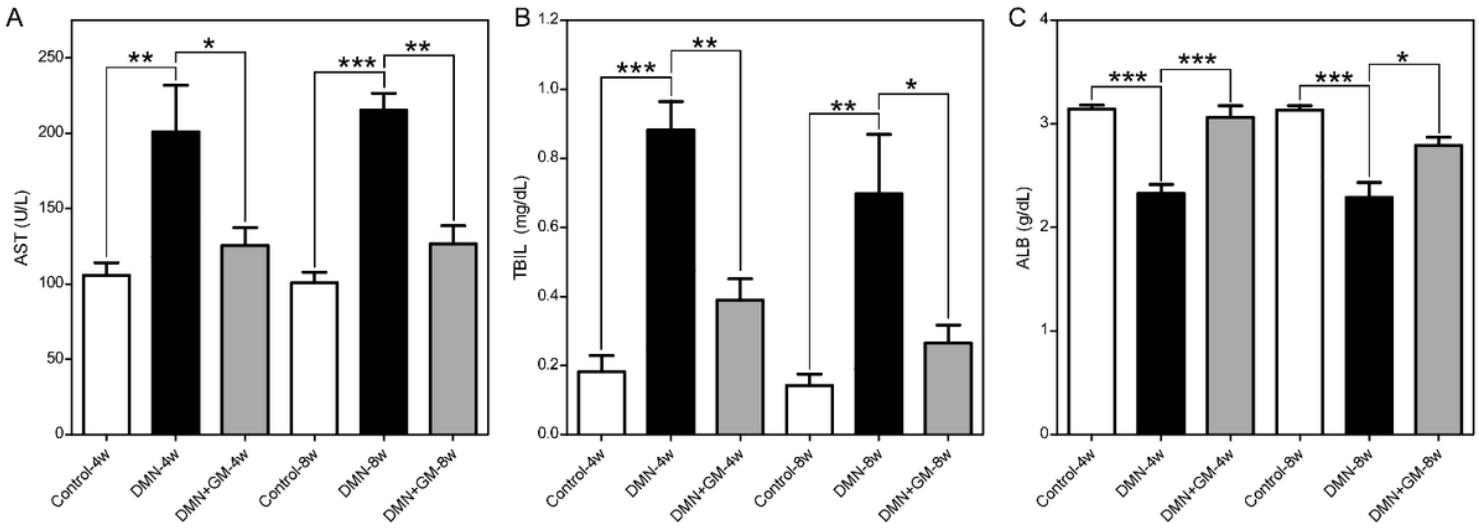

Figure 6

Effects of GM-CSF on DMN-induced hepatotoxicity in rats. Blood samples were collected from venous and arterial blood vessels and heart chambers after 4 or 8 weeks of DMN administration. Aspartate aminotransferase (AST), albumin (ALB), and total bilirubin (TBIL) were calculated from blood serum spectrometrically. Changes in serum AST (U/L) (A), TBIL (mg/dL) (B), and ALB (g/dL) (C) of rats treated with or without DMN ± GM-CSF for 4 and 8 week groups are given. Results are expressed as means ± SEM. Statistical significance was assigned as *** for $p \leq 0.001$, ** for $p \leq 0.01$, and * for $p \leq 0.05$.

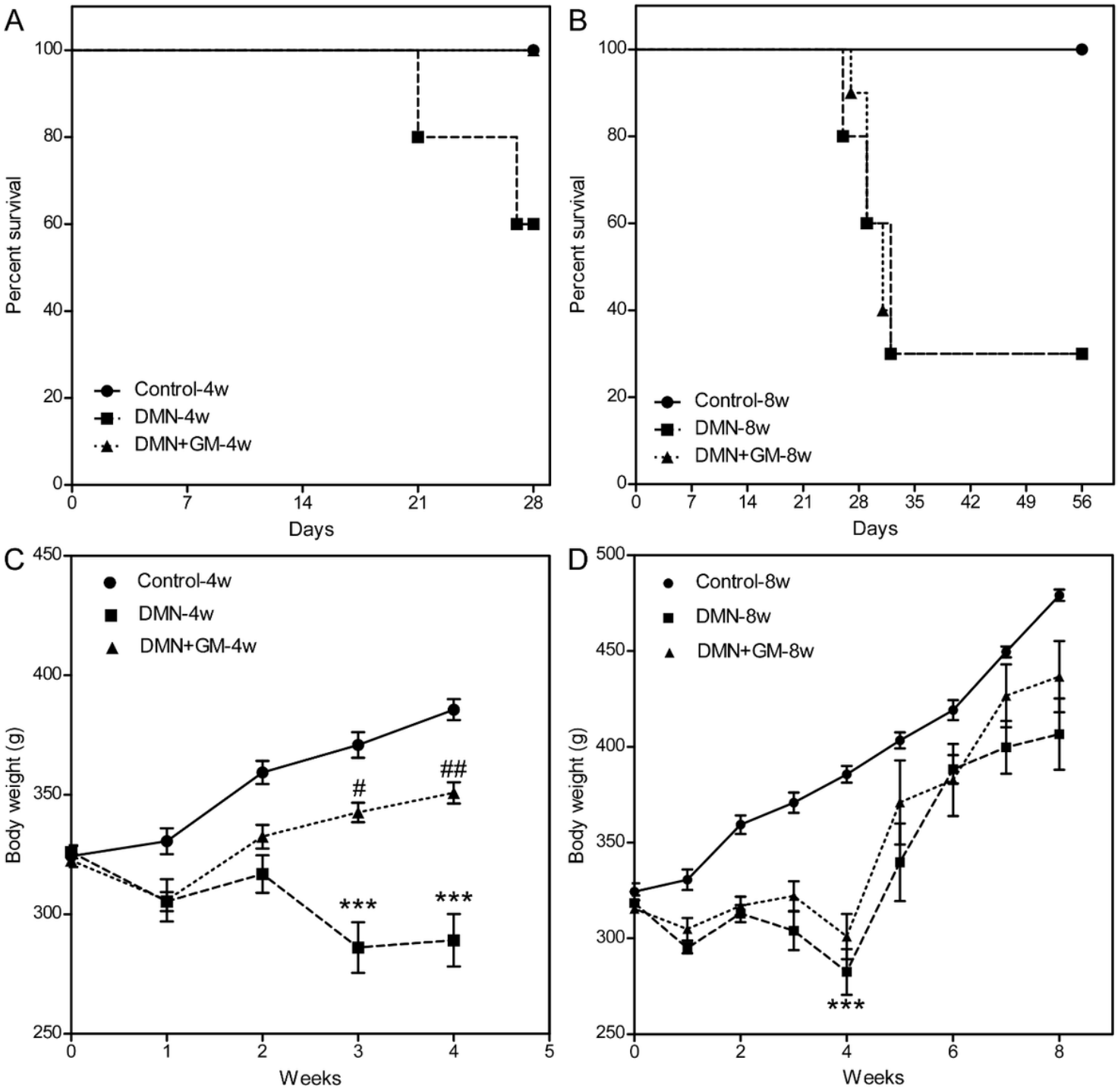

Figure 7

Effects of GM-CSF on DMN-induced changes in survival and body weights. Survival of rats are shown for the sham controls (n=10), DMN-treated (n=10), and DMN+GM-CSF-treated (n = 10) groups for 4-week (A) and 8-week groups (B). The death of rates was recorded every week and used to calculate survival rate. Body weights of rats are shown for the sham controls (n=10), DMN-treated (n=10), and DMN+GM-CSF-treated (n = 10) groups for 4-week (C) and 8-week group (D) rats. Body weights were measured weekly throughout the study. Results are expressed as means (± SEM). Statistical significance for the controls

vs. DMN-treated groups with or without GM-CSF are expressed as ## for p ≤ 0.01, # for p ≤ 0.05, and that for the DMN alone vs. DMN+GM-CSF-treated groups is expressed as *** for p ≤ 0.001.

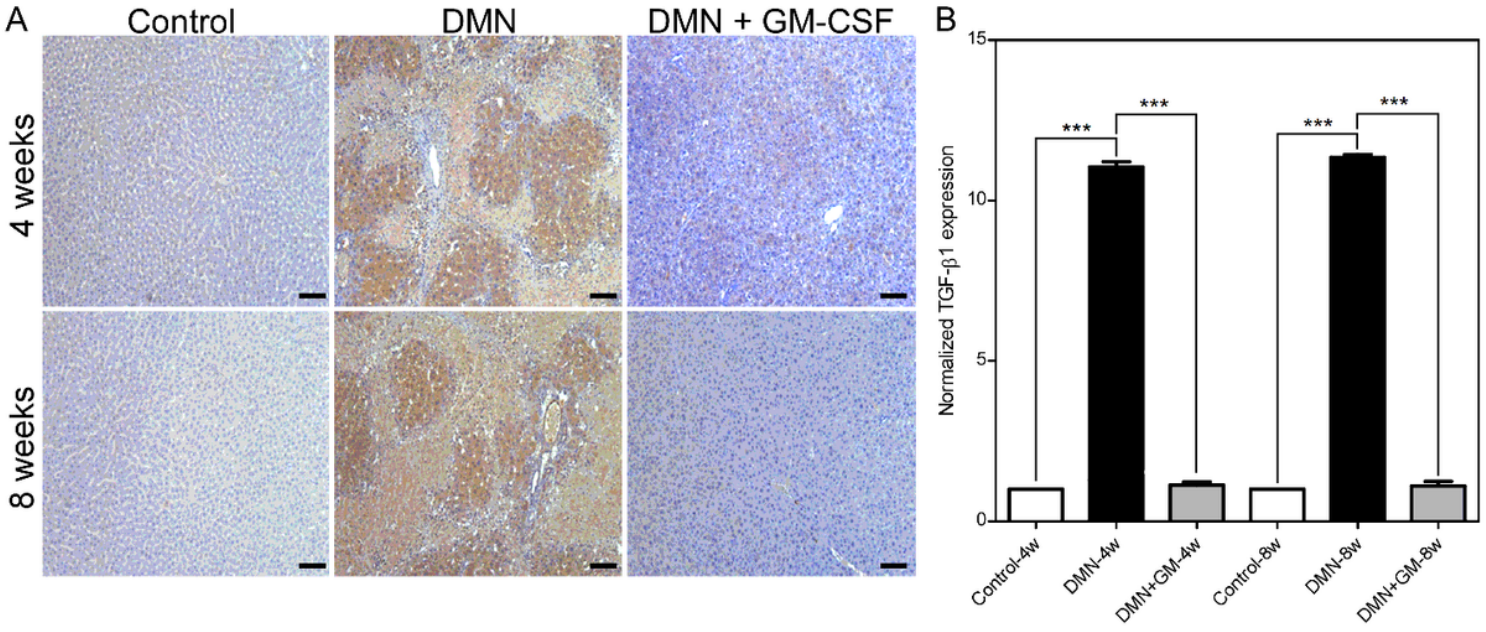

Figure 8

Effects of GM-CSF on DMN-induced TGF-β1 expression. (A) Representative images of immunohistochemical staining of TGF-β1 in controls, DMN-treated, and DMN+GM-treated groups for 4-week and 8-week treatment groups are shown. (B) Quantitative analysis of TGF-β1 expressions. Results are expressed as normalized means (± SEM) with respect to the controls. Statistical significance for the controls or DMN+GMCSF-treated groups vs. DMN-treated groups are expressed as *** for p ≤ 0.001.

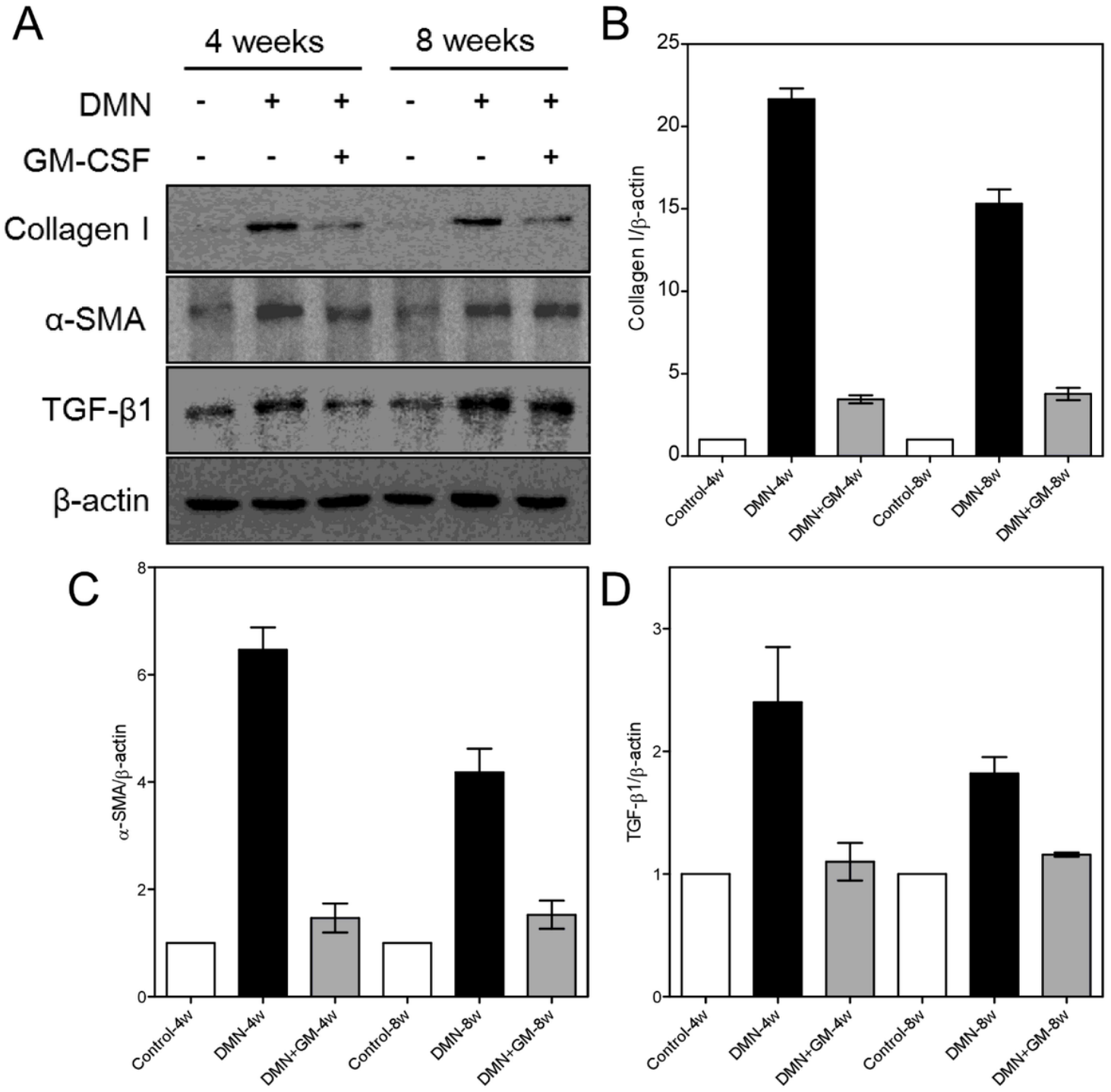

Figure 9

Expression of Collagen I, α-SMA, and TGF- β1 in the liver. (A) Protein expressions of Collagen I, α-SMA, and TGF- β1 by western blot method are shown. β-actin is used as the loading control. The gray density scanning analyses of (B) Collagen I, (C) α-SMA, and (D) TGF-β1 are shown. Results are expressed as means (± SEM). Statistical significance for the controls or DMN+GMCSF-treated groups vs. DMN-treated groups are expressed as *** for $p \leq 0.001$. The original images of the western blots for Collagen I, α-SMA, TGF-β1, and β-actin, developed in separate blots, were cropped and grouped together to prepare the figure.

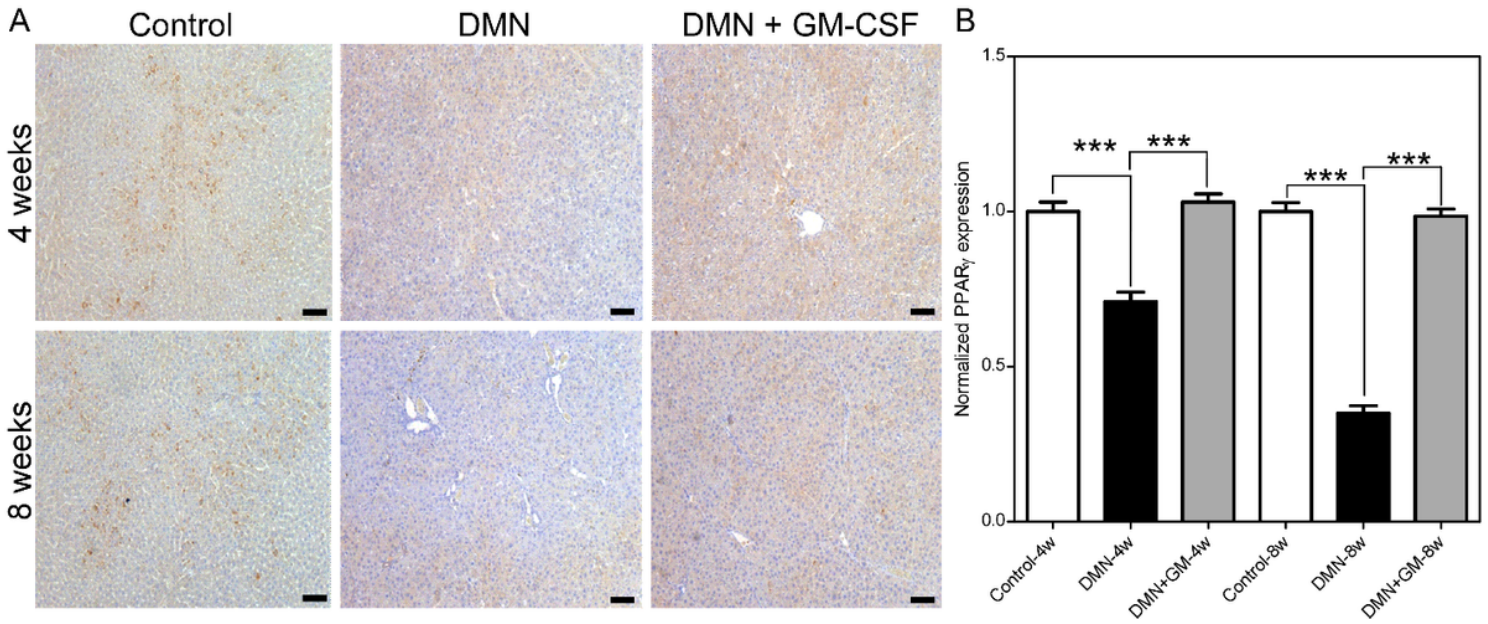

Figure 10

Effects of GM-CSF on DMN-induced inhibition of PPAR-γ expression. (A) Representative images of immunohistochemical staining of PPAR-γ in controls, DMN-treated, and DMN+GM-treated groups for 4-week and 8-week treatment groups are shown. (B) Quantitative analysis of PPAR-γ expressions. Results are expressed as normalized means (± SEM) with respect to the controls. Statistical significance for the controls or DMN+GMCSF-treated groups vs. DMN-treated groups are expressed as *** for $p \leq 0.001$.